Pressurized reversible operation of a 30-cell solid oxide cell stack using carbonaceous gases

Jensen, Søren Højgaard; Langnickel, Hendrik; Hintzen, N.; Chen, Ming; Sun, Xiufu; Hauch, Anne; Butera, Giacomo; Clausen, Lasse Røngaard

Published in:
Proceedings of the 7th European Fuel Cell Technology & Applications Conference (EFC2017)

Publication date:
2017

Document Version
Publisher's PDF, also known as Version of record

Proceedings of EFC2017
European Fuel Cell Technology & Applications Conference - Piero Lunghi Conference
December 12-15, 2017, Naples, Italy

EFC17255 EFC17

PRESSURIZED REVERSIBLE OPERATION OF A 30-CELL SOLID OXIDE CELL STACK USING CARBONACEOUS GASES

S. H. Jensen*, H. Langnickel*, N. Hintzen*, M. Chen*, X. Sun*, A. Hauch*, G. Butera**, L. R. Clausen**
*DTU Energy, Frederiksborgvej 399, 4000 Roskilde
**DTU Mechanical Engineering,
Nils Koppels Allé, B. 403, 2700 Lyngby
Technical University of Denmark

***Abstract* - Recent theoretical studies show that reversible electrochemical conversion of H_2O and CO_2 to CH_4 inside pressurized solid oxide cells (SOCs) combined with subsurface storage of the produced gases can facilitate seasonal electricity storage with a round-trip efficiency reaching 70-80% and a storage cost below 3 ¢/kWh. Here we show test results with a 30-cell SOFCMAN 301 stack operated with carbonaceous gases at 18.7 bar and 700 ˚C in both electrolysis and fuel cell mode. The CH_4 content in the stack outlet gas increased from 0.22% at open circuit voltage (OCV) to 18% at -0.17 A cm^{-2} in electrolysis mode. The degradation rates in both fuel cell and electrolysis mode were comparable to previously reported SOFCMAN stack degradation rates measured at ambient pressure operation with H_2/H_2O gas mixtures.**

***Index Terms* - Pressure, Internal, Methane, Efficiency, Storage**

I. Introduction

As intermittent wind and solar power displace fossil fuels the need increases for seasonal storage and production of transportation fuels. Power-to-gas (and fuels) is a relevant technology although the power-to-hydrogen conversion efficiency is rather low. Internal methanation in SOCs have been proposed to increase conversion and storage efficiency [1,2] and coupling with pressurized subsurface gas storage this could provide cost efficient large-scale electricity storage [3].

Catalytic CH_4 formation (and internal reforming) kinetics on a SOC fuel electrode have previously been studied at single-cell level at open circuit voltage (OCV) and ambient pressure [4] and recently at electrolysis conditions at pressures up to 10 bar [5]. It was found that CH_4 formation/reforming kinetics only to a limited degree influence the outlet gas composition.

The internal methane formation/reforming presented here suggests that kinetics to some extent influences the CH_4 content in the outlet gas, but other factors such as flow uniformity and internal leaks play a significant role.

II. Experimental

An SOFCMAN 301 stack with 30 NiO-YSZ/YSZ/CGO /LSCF-CGO cells [6,7] having 63 cm^2 active electrode area per cell was operated in a dedicated pressure test setup. The stack design is outlined in Fig. 1. The test setup is sketched in Fig. 2 and described in detail elsewhere [8].

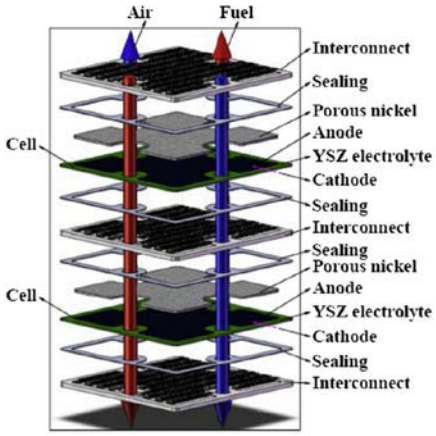

Fig. 1. Sketch of the internal structure in a 30-cell SOFCMAN. Figure taken from reference [9]

First the stack was heated to 750 ˚C followed by reduction of the NiO in the fuel electrodes. Subsequently the temperature was reduced to 700 ˚C. The remaining stack test is divided in four consecutive parts. Gas compositions for the central measurements in each part are specified in Table I.

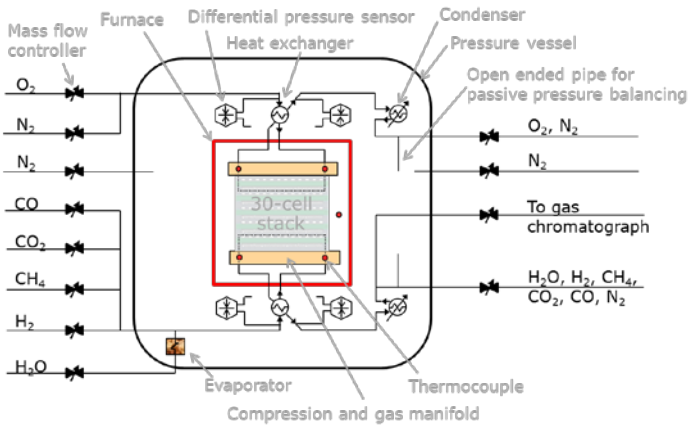

Fig. 2. Test setup used for pressurized operation of a 30-cell stack from SOFCMAN.

The central measurements in each part of the test are briefly described below.

Part A: The pressure was increased in four steps from 1 to 18.7 bar. Impedance spectra and iV curves were recorded at each step. The pressure drop across the stack and heat exchangers was measured during pressurization.

Part B: An equilibrium fuel gas mixture (neglecting higher hydrocarbons than CH_4) with an H/C ratio of 7 was fed to the stack. The inlet composition, and the outlet composition at OCV, -0.09 A cm^{-2} and -0.17 A cm^{-2} was measured with an Agilent micro GC 490 with a Molsieve 5Å and a PoraPlot Q column. Helium was used as carrier gas.

Part C: The oxygen concentration at the air side was reduced to minimize oxygen leaking from the air side to the fuel side. Subsequently the stack was operated at -0.10 A cm^{-2} for about 100 hours.

Part D: Next the stack was operated in fuel cell mode. Inlet gas composition, and the stack outlet gas composition was measured at OCV, 0.09 A cm^{-2} and 0.15 A cm^{-2}. The stack was operated at 0.09 A cm^{-2} for about 12 hours.

TABLE I
FUEL GAS FLOW RATE IN NORMAL LITERS PER HOUR DURING TEST

Test Part	*Fuel side*					*Air side*	
	H_2	H_2O	CO	CO_2	CH_4	O_2	N_2
A	200	200	0	0	0	126	474
B	31.5	140	6.2	36.8	1.3	126	474
C	31.5	140	6.2	36.8	1.3	40	1800
D	64.2	40.9	5.9	6.1	42.1	170	1800

III. RESULTS

The test results are presented with reference to the parts of the overall test outlined in Table I and discussed in Section II.

A. Pressure drop, iV and Impedance as Function of Pressure

In part A, the relative inlet and outlet pressure of both the fuel and oxidative gases was measured against the pressure in the autoclave using differential pressure sensors (Fig. 2). The difference between the inlet and outlet pressure is the pressure drop (dP) across the stack and heat exchangers (Fig. 3). The air flow to the stack was kept constant during the entire measurement whereas the fuel flow was varied above 3 bar.

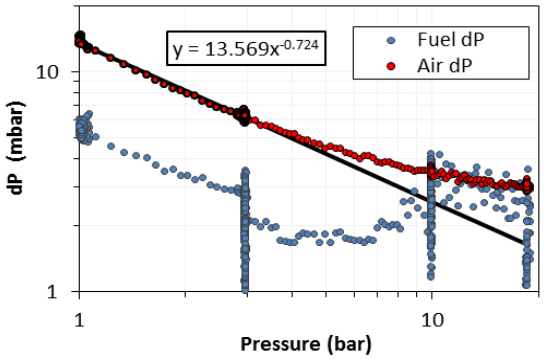

Fig. 3. Pressure drop across the SOFCMAN stack and heat exchangers as function of pressure. The air dP between 1 and 3 bar is fitted with a power law expression. The inset shows the power law expression.

The recorded iV curves are presented in Figure 4, *top*. Surprisingly the slope of the iV curves doesn't gradually decrease with increasing pressure. This is reflected by the average cell resistance (ASR), Fig. 4, *bottom*.

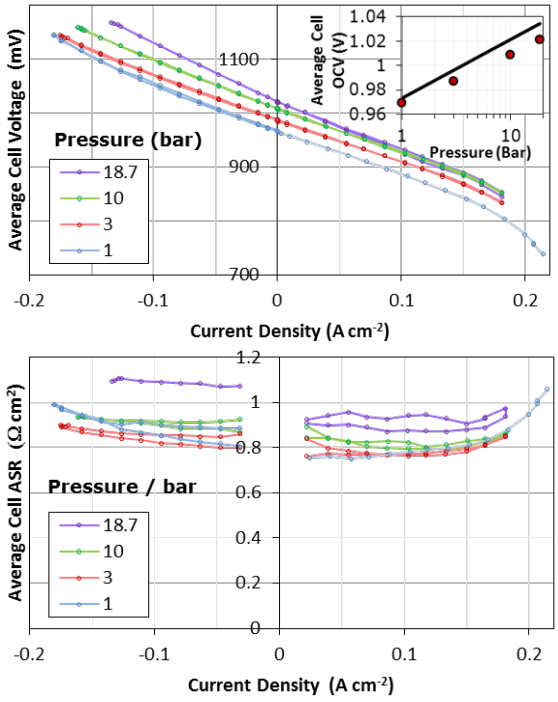

Fig. 4. *Top:* SOFCMAN stack iV curves recorded at various pressures. The inset show the OCV vs. pressure. The dots are measured stack OCV divided with the number of cells in the stack. The line is the theoretical Nernst cell voltage. *Bottom:* Average cell area specific resistance (ASR).

The average cell open circuit voltage (OCV) is shown in the inset in Fig. 4, *top*. Similar to previous stack tests, an increasing difference is observed with pressure between the theoretical cell OCV (the line) and the measured average cell OCV (the dots) [10]. The ASR is calculated as the absolute voltage difference between stack OCV and the stack voltage at the given current density, divided by the current density, and the number of cells in the stack.

Stack impedance spectra were recorded at OCV just before or after the iV curve measurements. The impedance spectra are presented in Fig. 5. Note how the size of electrode arc (high frequency part) decreases with increasing pressure. In contrast the Ohmic resistance seems to fluctuate with pressure.

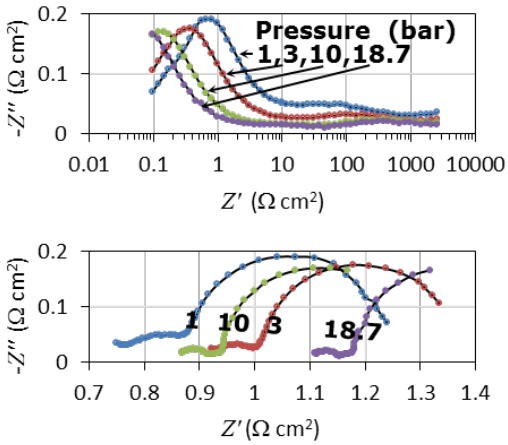

Fig. 5. *Top*: Bode plot. *Bottom*: Nyquist plot of impedance spectra recorded at 1,3,10 and 18.7 bar with the gas composition in Table I, part A.

B. Internal Methanation in the Stack

After the pressurization, iV and impedance measurements in test part A, the stack was operated with a carbonaceous gas to the fuel electrodes and air to the air electrodes (Table I, Test part B). The fuel inlet gas composition was the equilibrium composition, neglecting higher hydrocarbons than CH_4. The inlet gas composition was measured using the GC and used as calibration for the measurement of the outlet gas compositions.

The GC measurements revealed ~20 vol% N_2 in the stack fuel outlet gas. The dry gas composition corrected for the N_2 content is presented in the top part of Fig. 6. Importantly the measured CH_4 concentration in the outlet gas increased from 0.22 vol% at OCV to 18 vol% at -0.17 A cm^{-2}. The N_2 most likely entered the fuel gas from the air electrodes via seal and/or electrolyte leaks. The oxygen from the air leak will partially oxidize the fuel. In the bottom part of Fig. 6, the measured gas concentrations are corrected for the estimated fuel gas oxidation by shifting the measurement points to the right on the x-axis. In the estimation of the leak it is anticipated that the oxygen content near the air side of the electrolyte is larger at high electrolysis current, thus causing a higher leak than at OCV. With the applied correction for the internal leak it is observed that the outlet gas approximately reaches the equilibrium composition before it exits the stack. Arguably a part of the measured deviation from equilibrium concentration also relates to kinetic limitations of the methane formation, although this deviation is expected to be of less importance [4,5]. This is further discussed in Section IV.

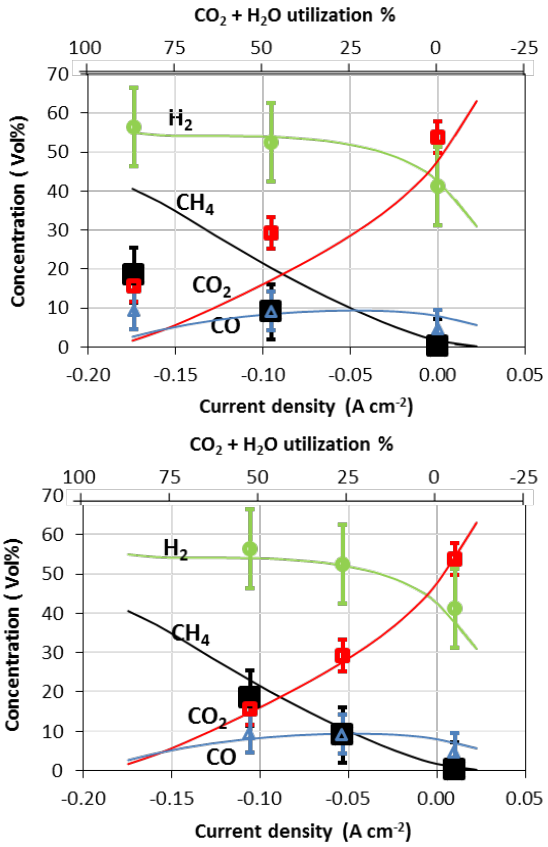

Fig. 6. *Top*: Measured gas composition (dots) as function of electrolysis current density. *Bottom*: Same gas compositions as above but shifted on the x-axis to correct for an internal leak in the stack. Lines represent the equilibrium concentration. Uncertainty bars reflect the GC measurement uncertainty.

C. Long-term Electrolysis Test

A substantial increase in the internal leak in the stack was observed after the measurements presented in Fig. 6. In order to continue the stack test the oxygen concentration at the air side was reduced to minimize oxygen leaking to the fuel side.

In part C, the stack voltage was measured as function of electrolysis test time (Fig. 7). During the test, the stack was exposed to a pressure cycle. The pressure cycle did not affect the stack OCV (not shown) and the stack voltage reached the same level as before the pressure cycle after a few hours of operation at -0.10 A cm^{-2}. The stack voltage as function of time gradually increased at a rate of 14% per 1000 hours (green line in the figure).

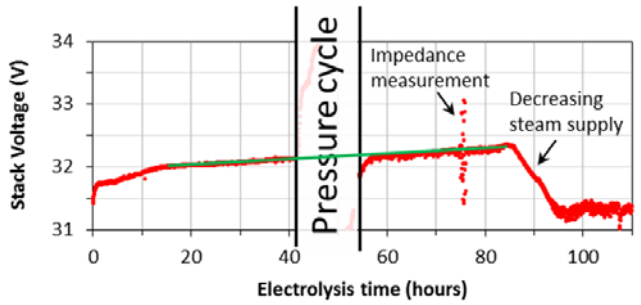

Fig. 7. Stack voltage during electrolysis operation at -0.10 A cm^{-2}. operated with the gas flow rates specified in test part C, Table I. At the end, the steam supply gradually decreased to 84 NLH.

At the end of test part C, a decreasing steam supply resulted in a decreasing stack voltage. At the same time the fuel gas inlet and outlet temperature increased as shown in Fig. 8.

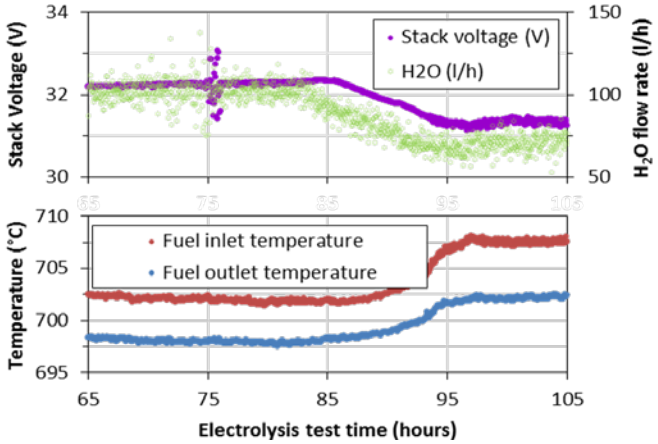

Fig. 8. *Top*: Stack voltage and steam flow rate during the last part of the electrolysis test presented in Fig. 7. *Bottom*: Fuel gas inlet and outlet temperature vs. test time.

D. Fuel Cell Operation and Internal Methane Reforming

After the electrolysis operation presented in Fig. 7 and 8, the stack was operated in fuel cell mode at 0.09 A cm^{-2} and 18.7 bar with a methane-rich gas specified in Table I, part D. The stack voltage as function of time is shown in Fig. 9. After the first five hours of operation the stack exhibited a degradation rate of 3.2% per 1000 hours (green line in Fig. 9).

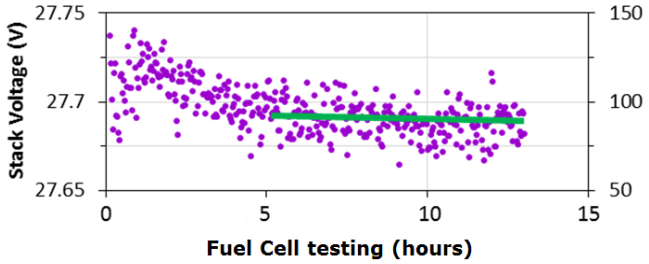

Fig. 9. Stack voltage as function of time at 0.09 A cm^{-2} and 18.7 bar operated with the gases shown in Table I, part D.

The stack inlet and outlet gas composition at OCV was measured prior to the measurements presented in Fig. 9. The outlet gas was measured at 0.09 A cm^{-2} and 0.15 A cm^{-2} respectively during, and immediately after, the voltage measurements presented in Fig. 9. The gas concentration as function of current density is presented in Fig. 10 and confirms a decreasing CH_4 and increasing CO_2 concentration with increasing fuel cell current density.

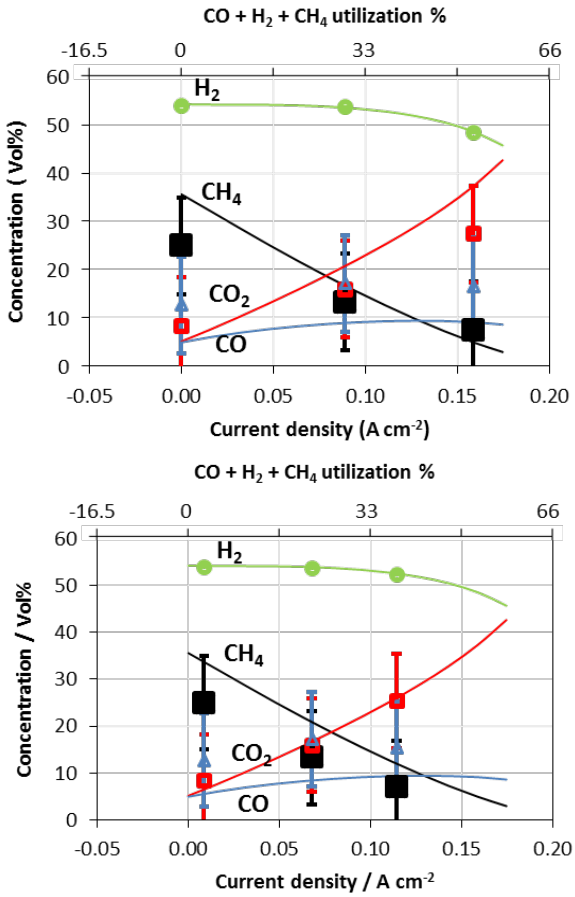

Fig. 10. *Top*: Measured gas composition (dots) as function of fuel cell current density. *Bottom*: Same gas compositions as above but shifted on the x-axis to correct for internal leaks in the stack and adjusted for the calculated H_2 concentration. The lines represent the equilibrium concentrations for the individual gases. Uncertainty bars reflect the GC measurement uncertainty. No uncertainty bars are given for the H_2 concentrations since it is a calculated equilbrium concentration and not a meaured concentration.

Due to a very high uncertainty for the H_2 concentration measurements, the presented H_2 concentration is not the measured concentration but the equilibrium concentration. This impacts the presented normalized concentrations for the remaining gases since the sum of the presented concentrations is normalized to 100%. Consequently this increases the uncertainties which are reflected in the relatively large uncertainty bars.

IV. Discussion

A. Pressure drop, iV and Impedance as Function of Pressure

In Fig. 3 a continuously decreasing pressure drop with increasing pressure is observed for the air side. The air flow to the stack was kept constant during the entire measurement whereas the fuel flow was varied above 3 bar. Further, the fluctuations in the fuel side dP above 3 bar is most likely caused by condensation in the differential pressure sensor pipes. The iV curve measurements considerably affect the fuel dP due to the change in H_2/H_2O concentration in the stack outlet gas via the mentioned condensation.

The air pressure drop doesn't follow a straight line indicating the pressure drop deviates from an isentropic pressure drop across the stack and heat exchangers [8,10]. An isentropic air pressure drop theoretically exhibits an exponent of -0.71 [10]. The fit in Fig. 3 show an exponent of -0.724, i.e. in relatively good agreement with theory. The deviation from the straight line above 3 bar is possibly related to a decreasing flow uniformity in the stack with increasing pressure [11]. Additionally, the air in the corners of each cell is likely more stagnant at high pressure than at low pressure [12] which would also decrease the measured exponent. CFD calculations could be used to investigate this further, but is beyond the scope of this paper.

The lower dP at high pressure enables operation of stacks with larger foot prints since more gas can pass the gas channels at a certain maximum allowable pressure drop in the gas channels. In fact, to a first approximation the cell side length scales with the square root of the pressure [10]. This means that if the maximum cell side length achievable today in planar SOC stacks is ~20 cm, it could be ~100 cm at 25 bar, thereby truly enabling MW SOC stacks!

The OCV in the inset in Fig. 4, *top* shows an increasing difference with increasing pressure between the Nernst cell voltage and the measured average cell OCV. This is previously observed, and assigned to electrolyte pin-holes and/or gas leaks at the internal stack manifolds [8,10]. The result emphasizes the importance of a careful minimization of gas leaks at the electrolytes and manifolds when designing stacks for pressurized operation. It should be noted that to some extent low flow uniformity could also lower the measured average cell OCV.

As opposed to previous stack tests the ASR did not systematically decrease with increasing pressure, Fig. 4, *bottom*. This is most likely related to the changes in the Ohmic part of the impedance (Fig. 5, *Bottom*). The change in Ohmic part of the impedance is possibly related to loss of (electric) contact at the various interfaces of the fuel side components (Fig. 1). It is currently not known what caused the loss of contact during pressurization, but thermo-mechanical stress could be an explanation.

It should be noted that the interception of the gas conversion arc with the x-axis in Fig. 5, *Bottom* is substantially larger than the ASR measured at low current densities (Fig. 4, *Bottom*). This is possibly due to an inaccurate measurement of the impedance shunt resistance. Importantly, the relative size of the four measured impedance spectra is believed to be correct.

Similar to previous tests the summit frequency f_s of the gas conversion arc (low freq. part, Fig 5, *top*) decreases with increasing pressure [8,10]. The summit frequency vs. pressure is presented in Fig. 11.

Based on the ideal gas law, a P^{-1}-depencency of the summit frequency of the gas conversion arc is previously predicted for the fuel electrode [13]. A similar continuous stirred-tank reactor (CSTR)-model would predict a P^{-1}-depencency for the summit frequency of the oxygen (in air) conversion arc at the air-electrode. The fit shows an exponent of -0.753. This is lower than the -0.90 exponent value obtained with a previous stack test [10]. The reason for the deviation from -1 is possibly related to decreasing gas flow-uniformity with increasing pressure, i.e. higher flow rates at some cells than others, and stagnant gas in cell corners. A detailed CFD analysis of the gas flow inside the stack could help quantifying this, but is beyond the scope of this paper.

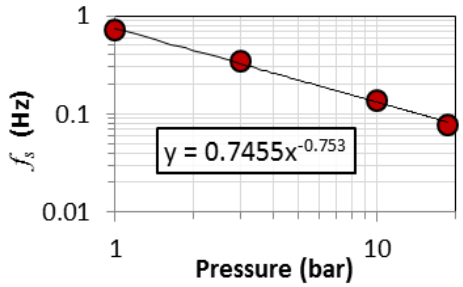

Fig. 11. Summit frequency f_s as function of pressure. The line represents the best fit using the expression in the figure.

The resistance related to gas conversion and binary gas diffusion is predicted to be independent of pressure [13,14]. As expected the size of the gas conversion arc (Fig 5, *bottom*) is seen to be relatively independent of pressure.

B. Internal Methanation in the Stack

The methane concentration in the stack outlet gas clearly increases with increasing pressure, Fig.6. Unfortunately the stack voltage was not stable during operation at -0.17 A cm^{-2}. After ~2 hours of operation the current was switched off. Subsequently the OCV had dropped significantly indicating substantial increase in the internal leaks. This is possibly related to a low flow uniformity combined with a high total CO_2 and H_2O utilization of 88% at -0.17 A cm^{-2}. The operation conditions (700 ˚C, 18.7 bar, and a H/C ratio = 7) should not result in carbon formation – even with a local utilization approaching 100%. However, if the utilization exceeds 100%

the YSZ may be reduced which can permanently damage the cells. Further, the higher diffusivity of H_2 relative to that of H_2O, CO, CO_2, and CH_4 could possibly decrease the H/C ratio near the triple phase boundaries in the fuel electrode, which again could cause local carbon formation. Post Mortem SEM microscopy of the stack can hopefully help determining if coking or YSZ reduction occurred in the fuel electrodes.

It is not clear to what extent the lower methane content relative to equilibrium content is caused dominantly by oxidation of the fuel due to internal leaks or by kinetic limitations of the methane formation. However, at OCV the methane content in the outlet gas was 0.22% i.e. less than the (dry) equilibrium concentration of 1.7 %. This indicates that oxidation of the fuel gas via internal leaks in the stack substantially decreased the methane concentration. Besides the substantial amount of micron-scale Ni-particles in the fuel electrodes and cell supports, the SOFCMAN stack is equipped with Ni foam components (Fig. 1) which provides additional catalyst area for the methane formation.

C. Long-term Electrolysis Test

The constant current electrolysis operation exhibited a gradual stack voltage increase corresponding to a 14% kh^{-1} degradation rate. This is comparable to a degradation rate of ~12% kh^{-1} for an SOFCMAN 30-cell stack tested at -0.15 A cm^{-2} and 800 ˚C in a H_2/H_2O mixture [7]. The referenced SOFCMAN stack had LSM-YSZ air electrodes whereas the tested stack had cells with LSCF-YSZ electrodes. The difference in electrodes, operation temperature and in current density clearly affects the degradation rate. Despite the high uncertainty it is encouraging that relative to ambient pressure steam electrolysis, pressurized operation with internal methane formation seems to have limited impact on the degradation rate.

At the end of the constant-current operation, the steam supply gradually decreased. If the stack had been operating on a pure H_2O/H_2 mixture, decreasing steam content would have increased the stack voltage. Instead the stack voltage started to decrease. When the stack voltage decreases the electrolysis operation becomes increasingly endothermic and this would decrease the gas inlet and outlet temperature. Contrary to this, the gas inlet and outlet temperature increased when the steam supply decreased. With a decreasing steam supply, the equilibrium methane concentration increases which again make the overall reaction more exothermic. This will increase the inlet and outlet gas temperature (the former via the heat exchanger).

D. Fuel Cell Operation and Internal Methane Reforming

The constant current fuel cell operation shows a degradation rate of 3.2% kh^{-1}. Despite the high uncertainty on the estimation of the degradation rate due to the short test period, it is interesting to compare it with degradation rates measured at ambient pressure. A degradation rate of 2.3% kh^{-1} have been reported for a 5-cell SOFCMAN stack equipped with Ni-YSZ/YSZ/LSC-YSZ cells when operated at ambient pressure, 700 ˚C and 0.4 A cm^{-2}, and with H_2 and air to the fuel and air electrodes respectively [9]. Obviously, the higher current density and the different air electrodes hamper a direct comparison of the degradation rates. Nevertheless, it is encouraging that the operation with a methane rich equilibrium gas show comparable low degradation rates.

Although the GC measurements are very uncertain it is clear that the CH_4 concentration decreases with increasing fuel cell current density. The CH_4 concentration seems to decrease less with increasing current density than what would be expected if the gas reached equilibrium. This could indicate that CH_4 reforming kinetics to some extent limit the conversion and full equilibration is not obtained.

V. Conclusion

Internal CH_4 formation and reforming in solid oxide fuel cells can potentially enable system conversion efficiencies (power-to-gas-to-power) reaching 70-80%. When operating an SOFCMAN 30-cell stack with a carbonaceous gas equilibrated at 700 ˚C and 18.7 bar, the CH_4 concentration in the stack outlet gas (after condensation of H_2O) increased from 0.22% at OCV to 18% at -0.17 A cm^{-2}. The outlet gas did not fully reach equilibrium. This is most likely related to partial oxidation of the fuel gas due to leaks in the stack and limiting methane formation kinetics.

Impedance spectra recorded during pressurization indicates loss of contact inside the stack during pressurization. The cause of the contact loss is unknown, but thermo-mechanical stress could be an explanation.

The air pressure drop across the stack and heat exchangers increasingly deviates from an isentropic pressure drop above 3 bar. This indicates decreasing flow uniformity with increasing pressure. The gas conversion summit frequency obtained from the impedance spectra decreases with $P^{-0.753}$, where P is the total absolute gas pressure. The absolute value of the exponent is substantially smaller than 1, which further indicates limited flow uniformity at the higher pressures.

Fuel cell operation with a CH_4 rich carbonaceous gas equilibrated at 700 ˚C and 18.7 bar shows a decrease in the CH_4 concentration when increasing the current density from 0 A cm^{-2} to 0.15 A cm^{-2}, thus confirming internal methane reforming.

Although the test period in both electrolysis and fuel cell modes was rather short, the estimates of the degradation rates seem comparable with ambient pressure degradation rates.

Acknowledgment

The authors acknowledge financial funding from the Energy

Technology Development and Demonstration Program (EUDP) via project no. 64015-0523 “Maturing SOEC”. The authors wish to thank Bent Førster Hansen, Jens Østergaard, Jens Borchsenius, John Johnson, Martin Nørby Nielsen and Søren Koch for technical expertise and assistance in developing the test setup and running the test.

REFERENCES

[1] D. M. Bierschenk, J. R. Wilson, S. A. Barnett, High efficiency electrical energy storage using a methane-oxygen solid oxide cell, *Energy Environ. Sci.*, **4** 944 (2011).

[2] S. H. Jensen, M. Mogensen, Perspectives of high temperature electrolysis using SOEC, *in* 19th World Energy Congress, September 5-9, Sydney, AU, 2004

[3] S.H. Jensen, C. Graves, M. Mogensen, C. Wendel, R. Braun, G. Hughes, Z. Gao, S.A. Barnett, Large-scale electricity storage utilizing reversible solid oxide cells combined with underground storage of CO_2 and CH_4, *Energy Environ. Sci.*, **8** 2471 (2015)

[4] H. Timmermann, W. Sawady, R. Reimert, E. Ivers-Tiffée, Kinetics of (reversible) internal reforming of methane in solid oxide fuel cells under stationary and APU conditions, *J. Power Sources*, **195** 214 (2010)

[5] L. Bernadet, J. Laurencin, G. Roux, D. Montinaro, F. Mauvy, M. Reytier, Effects of Pressure on High Temperature Steam and Carbon Dioxide Co-electrolysis, *Electrochimica Acta*, *Accepted*, http://dx.doi.org/10.1016/j.electacta.2017.09.037

[6] W. Guan and W. Wang, Electrochemical Performance of Planar Solid Oxide Fuel Cell (SOFC) Stacks: From Repeat Unit to Module, *Energy Technol.*, **2**, 692 (2014)

[7] Y. Zheng,Q. Li,W. Guan,C. Xu, W. Wu, W. Wang, Investigation of 30-cell solid oxide electrolyzer stack modules for hydrogen production, *Ceramics Int.*, **40** 5801 (2014)

[8] S. H. Jensen, C. Graves, M. Chen, J. B. Hansen, X. Sun, Characterization of a Planar Solid Oxide Cell Stack Operated at Elevated Pressure, *J. Electrochem. Soc.*, **163** F1596 (2016)

[9] L. Jin, W. Guan, X. Ma, H. Zhai, W. Wang, Quantitative contribution of resistance sources of components to stack performance for planar solid oxide fuel cells, *J. Power Sources*, **253** 305 (2014)

[10] S. H. Jensen, X. Sun, S. D. Ebbesen and M. Chen, Pressurized Operation of a Planar Solid Oxide Cell Stack, *Fuel Cells*, **2**, 205 (2016)

[11] W. Bi, D. Chen, Z. Lin, A key geometric parameter for the flow uniformity in planar solid oxide fuel cell stacks. *Int. J. Hydrogen Energy*, **34** 3873 (2009)

[12] R. J. Kee, P. Korada, K. Walters, M. Pavol, A generalized model of the flow distribution in channel networks of planar fuel cells. *J. Power Sources*, **109** 148 (2002)

[13] S. Primdahl, M. Mogensen, Gas Conversion Impedance: A Test Geometry Effect in Characterization of Solid Oxide Fuel Cell Anodes, *J. Electrochem. Soc.*, **145** 2431 (1998)

[14] S. Primdahl, M. Mogensen, Gas Diffusion Impedance in Characterization of Solid Oxide Fuel Cell Anodes, *J. Electrochem. Soc.*, **146** 2827 (1999)